Decoherence of coupled Josephson charge qubits due to partially correlated low-frequency noise

Yong Hu,* Zheng-Wei Zhou,† Jian-Ming Cai, and Guang-Can Guo
Key Laboratory of Quantum Information, University of Science and Technology of China, Chinese Academy of Sciences, Hefei, Anhui 230026, China

(Received 26 March 2007; published 21 May 2007)

Josephson charge qubits are promising candidates for scalable quantum computing. However, their performances are strongly degraded by decoherence due to low-frequency background noise, typically with a $1/f$ spectrum. In this paper, we investigate the decoherence process of two Cooper pair boxes (CPBs) coupled via a capacitor. Going beyond the common and uncorrelated noise models and the Bloch-Redfield formalism of previous works, we study the coupled system's quadratic dephasing under the condition of partially correlated noise sources. Based on reported experiments and generally accepted noise mechanisms, we introduce a reasonable assumption for the noise correlation, with which the calculation of multiqubit decoherence can be simplified to a problem on the single-qubit level. For the conventional Gaussian $1/f$ noise case, our results demonstrate that the quadratic dephasing rates are not very sensitive to the spatial correlation of the noises. Furthermore, we discuss the feasibility and efficiency of dynamical decoupling in the coupled CPBs.

DOI: 10.1103/PhysRevA.75.052327 PACS number(s): 03.67.Lx, 03.67.Pp, 85.25.Cp

I. INTRODUCTION

One of the most serious obstacles towards implementing charge-based superconducting quantum computing (QC) [1,2] is low-frequency charge noise [3]. During the past few years, the decoherence dynamics of a single Cooper pair box (CPB) exposed to Gaussian $1/f$ noise or random telegraph noise (RTN) [4] has been studied extensively [5–7]. In both circumstances, the free induction decay (FID) and echo law at an arbitrary working point have already been obtained. In addition, to preserve the single qubit's quantum coherence, various elegant ideas, including optimal point operation [8], bang-bang control [3,9], and decoherence free subspace (DFS) encoding [10,11], have been developed.

Stimulated by these advances, recently attention has been paid to the dissipation of coupled qubits [12–17]. The main motivation is to facilitate the physical realization of universal QC. Compared with its single-qubit counterpart, the analysis of multiqubit decoherence becomes much more difficult. As two extreme cases, coupled qubits in the presence of two common and uncorrelated noise sources [12,13] have been investigated within the Bloch-Redfield formalism [18]. The interaction between many qubits and a common harmonic bath with different coupling strengths has also been discussed in the context of quantum dots [14]. Very recently, Tsomokos *et al.* have considered the entanglement dynamics in chains of Josephson qubits with spatially uncorrelated noise [17].

In charge-type Josephson junction nanodevices, a part of the charge fluctuations results from the finite impedance of the external control coil and the residual coupling from the measurement apparatus. In most scenarios, this part of the noise is nearly white with Gaussian statistics. It can thus be well understood within the spin-boson model [19] and the Bloch-Redfield equations. However, the main part of the charge fluctuations is the low-frequency background noise, which is believed to be produced by the ensemble of charged two-level fluctuators (TLFs) distributed in the oxide barriers of the Josephson junctions as well as the dielectric substrate [4,20]. The low-frequency noise is often long-range correlated in time with a zero-frequency peak in its power spectrum. Due to this property, the background noise has little effect on the depolarization process but dominates the dephasing of charge qubits [5,7].

Therefore we can see there are still stumbling blocks in applying previous approaches to characterize the decoherence of coupled charge qubits. First of all, as indicated by experiments [20], neither the common bath nor the uncorrelated bath can fully describe the realistic environment. Moreover, as a kind of Fermi golden rule theory, the Bloch-Redfield formalism is valid only if the noise is weakly coupled to the system and has a short correlation in time. In more general situations, such as $1/f$ noise or a few very strong RTNs [21,22], the Bloch-Redfield theory breaks down and higher-order correction is necessary [5,7,23].

Based on these issues, in this paper we aim at calculating the quadratic dephasing effect of two coupled CPBs [24,25] caused by two partially correlated low-frequency noise sources. To handle the partial correlation of noise sources, we introduce a linear cross approximation (LCA) which is supported by the present reported experimental data and the widely accepted Dutta-Horn model [4] of low-frequency noise. The LCA states that the cross spectrum of two noise sources has the same form as their individual power spectra [20]. With this approximation, the task of evaluating the dephasing of coupled CPBs can be reduced to resolving a single qubit's dissipation. Our numerical results imply that the quadratic dephasing depends weakly on the spatial correlation of the noises. Furthermore, we also consider the application of dynamical decoupling techniques in this coupled system.

This paper is organized as follows. In Sec. II we express the model of the coupled CPBs and the noise sources. In Sec.

*Electronic address: yhu3@mail.ustc.edu.cn
†Electronic address: zwzhou@ustc.edu.cn

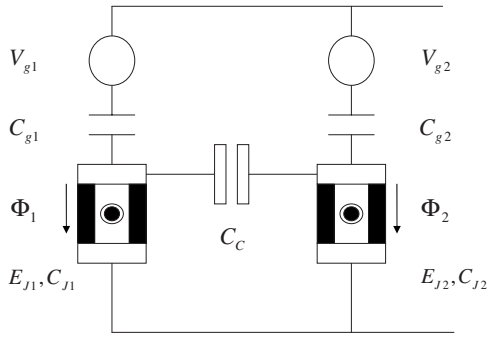

FIG. 1. Schematic plot of two capacitively coupled Josephson charge qubits.

III, we first review the LCA with a detailed explanation of its physical meaning, and then we use it to derive the FID law of the system's density matrix. In Sec. IV we discuss how to realize the dynamical decoupling in the coupled-qubit system. The numerical simulations of decoherence rates are presented in Sec. V, while the discussion and conclusion are made in Sec. VI.

II. SYSTEM CHARACTERIZATION

We start with two capacitively coupled CPBs [26,24,25], as sketched in Fig. 1. Each CPB consists of a small superconducting island with n_i excess Cooper pairs, connected to the ground electrode by a symmetric superconducting quantum interference device with capacitance C_{Ji} and tunable Josephson coupling energy E_{Ji} [27], for $i=1,2$. The gate voltages V_{gi} bias the corresponding CPBs via the gate capacitors C_{gi}. Finally, the CPBs are connected to each other by a coupling capacitor C_c. The Hamiltonian of the coupled system reads [28]

$$H_S = 4E_m(n_1 - n_{g1})(n_2 - n_{g2}) + \sum_{i=1,2} [E_{ci}(n_i - n_{gi})^2 + E_{Ji}\cos\Phi_i], \quad (1)$$

where $n_{g1,2}=C_{g1,2}V_{1,2}/2e$ denote the gate-induced charge numbers on the corresponding qubits; $\Phi_{1,2}$ are the canonical conjugate variables to $n_{1,2}$; $E_{c1,2}=2e^2C_{\Sigma 2,1}/(C_{\Sigma 2,1}C_{\Sigma 1,2}-C_c^2)$ are the effective Cooper-pair charging energies ($C_{\Sigma i}=C_{gi}+C_{Ji}+C_c$ is the sum of all capacitances connected to the ith CPB); and $E_m=e^2C_c/(C_{\Sigma 2,1}C_{\Sigma 1,2}-C_c^2)$ is the inter-qubit capacitive coupling energy. Near the codegeneracy point $n_{g1}=n_{g2}=1/2$, one can use the two-level language [27,29,30]

$$n_i = (1+\sigma_{zi})/2, \quad \cos\Phi_i = \sigma_{xi}/2, \quad (2)$$

for $i=1,2$, to describe the system as

$$H_S = E_m\sigma_{z1}\sigma_{z2} + \frac{1}{2}\sum_{i=1,2}(E_{bi}\sigma_{zi} + E_{Ji}\sigma_{xi}), \quad (3)$$

where

$$E_{b1,2} = 2[E_{c1,2}(1-2n_{g1,2}) + E_m(1-2n_{g2,1})]. \quad (4)$$

Like other Coulomb blockade devices [31], the coupled CPBs are very sensitive to noise from charge degrees of freedom. Incorporating $\delta n_{gi}(t)$ as the fluctuations of the reduced offset charge n_{gi} for $i=1,2$, we rewrite the Hamiltonian Eq. (1) as

$$H_S = E_m\sigma_{z1}\sigma_{z2} + \frac{1}{2}\sum_{i=1,2}\{[E_{bi} + 2V_i(t)]\sigma_{zi} + E_{Ji}\sigma_{xi}\}, \quad (5)$$

where

$$V_{1,2}(t) = -2[E_{c1,2}\delta n_{g1,2}(t) + E_m\delta n_{g2,1}(t)]. \quad (6)$$

By operating the single qubit at the optimal point, chosen such that the linear longitudinal qubit-noise coupling vanishes, one can prolong the dephasing time by several orders of magnitude [8,9,32,33], thus making the observation of the detailed decoherence process possible. For this reason, here we concentrate only on the behavior of the system at the codegeneracy point $n_{g1}=n_{g2}=1/2$, which can be verified as the optimal point for the coupled qubits. At this point, we may use the local transformation of basis (for $i=1,2$, $|\uparrow\rangle_i$, and $|\downarrow\rangle_i$ are the eigenstates of n_{gi} with eigenvalues 0 and 1, respectively)

$$|\uparrow\rangle_i \to (|\uparrow\rangle_i + |\downarrow\rangle_i)/\sqrt{2},$$

$$|\downarrow\rangle_i \to (|\uparrow\rangle_i - |\downarrow\rangle_i)/\sqrt{2}, \quad (7)$$

to transform the total Hamiltonian H_S to

$$H_S' = H_0 + H_1, \quad (8)$$

with

$$H_0 = \frac{1}{2}(E_{J1}\sigma_{z1} + E_{J2}\sigma_{z2} + 2E_m\sigma_{x1}\sigma_{x2}), \quad (9)$$

$$H_1 = \sigma_{x1}V_1(t) + \sigma_{x2}V_2(t). \quad (10)$$

Without loss of generality, we consider identical qubits with $E_{J1}=E_{J2}=E_J$ and $E_{c1}=E_{c2}=E_c$. Defining $E=\sqrt{E_m^2+E_J^2}$ and $\cos 2\theta = E_J/E$, we get the representation of H_0 in its eigenbasis $\{|1\rangle=\cos\theta|\uparrow\uparrow\rangle+\sin\theta|\downarrow\downarrow\rangle$, $|2\rangle=-\sin\theta|\uparrow\uparrow\rangle+\cos\theta|\downarrow\downarrow\rangle$, $|3\rangle=(|\uparrow\downarrow\rangle+|\downarrow\uparrow\rangle)/\sqrt{2}$, $|4\rangle=(|\uparrow\downarrow\rangle-|\downarrow\uparrow\rangle)/\sqrt{2}\}$

$$H_0 = \begin{bmatrix} E & 0 & 0 & 0 \\ 0 & -E & 0 & 0 \\ 0 & 0 & E\sin 2\theta & 0 \\ 0 & 0 & 0 & -E\sin 2\theta \end{bmatrix}. \quad (11)$$

The operators $\sigma_{x1,2}$ through which the system couple to the environment have the matrix form

$$\sigma_{x1} = \begin{bmatrix} 0 & 0 & \sin\left(\theta+\frac{\pi}{4}\right) & -\cos\left(\theta+\frac{\pi}{4}\right) \\ 0 & 0 & \cos\left(\theta+\frac{\pi}{4}\right) & \sin\left(\theta+\frac{\pi}{4}\right) \\ \sin\left(\theta+\frac{\pi}{4}\right) & \cos\left(\theta+\frac{\pi}{4}\right) & 0 & 0 \\ -\cos\left(\theta+\frac{\pi}{4}\right) & \sin\left(\theta+\frac{\pi}{4}\right) & 0 & 0 \end{bmatrix}, \tag{12}$$

$$\sigma_{x2} = \begin{bmatrix} 0 & 0 & \sin\left(\theta+\frac{\pi}{4}\right) & \cos\left(\theta+\frac{\pi}{4}\right) \\ 0 & 0 & \cos\left(\theta+\frac{\pi}{4}\right) & -\sin\left(\theta+\frac{\pi}{4}\right) \\ \sin\left(\theta+\frac{\pi}{4}\right) & \cos\left(\theta+\frac{\pi}{4}\right) & 0 & 0 \\ \cos\left(\theta+\frac{\pi}{4}\right) & -\sin\left(\theta+\frac{\pi}{4}\right) & 0 & 0 \end{bmatrix}. \tag{13}$$

III. QUADRATIC DEPHASING AND THE SPATIAL CORRELATION OF NOISE SOURCES

In general, the transverse noises $V_1(t)$ and $V_2(t)$ lead to relaxation through the nondiagonal entries of σ_{x1} and σ_{x2}. However, due to their low-frequency properties, the effect of quadratic dephasing becomes comparable with, or even more severe than, the relaxation process [5,7]. The physical picture of the quadratic dephasing can be imagined as follows. The low-frequency charge noise slowly and randomly drifts the system away from its initial bias point; then the system's quantum state will follow the drift adiabatically. During this adiabatic process, each eigenstate will get a very small energy shift to the second-order approximation; thus an additional random phase is accumulated. Since the depolarization process and the quadratic dephasing can be treated in a factorized way [9,23], in the rest of this paper we calculate the latter effect.

In realistic CPB implementations [8,9,24,25], E is often of the order of 20 GHz, while the coupling strength $E\sin 2\theta$ is usually smaller than E by one order of magnitude; a typical choice $C_c=0.09C_\Sigma$ and $E_J=E_c$ leads to $\sin 2\theta \cong 0.042$; thus $E\sin 2\theta$ is on the level of a few gigahertz; in addition, for $i=1,2$ the strength of the dimensionless noise δn_{gi} is usually on the level of 10^{-3} [9]. Therefore, near the optimal point, the eigenenergies of H_S can be derived by the second-order perturbation theory:

$$E_i = E_{i0} + \alpha_i q_1^2(t) + \beta_i q_2^2(t), \tag{14}$$

with

$$q_1(t) = [V_1(t) + V_2(t)]/\sqrt{2},$$

$$q_2(t) = [V_1(t) - V_2(t)]/\sqrt{2}, \tag{15}$$

where E_{i0} are the unperturbed eigenenergies of state $|i\rangle$ for any i and the coefficients α_i, β_i are

$$\alpha = \frac{(1+\sin 2\theta)}{E(1-\sin 2\theta)}, \quad \beta = \frac{(1-\sin 2\theta)}{E(1+\sin 2\theta)},$$

$$\alpha_1 = \alpha, \quad \beta_1 = \beta, \quad \alpha_2 = -\beta, \quad \beta_2 = -\alpha,$$

$$\alpha_3 = -\alpha+\beta, \quad \beta_3 = 0, \quad \alpha_4 = 0, \quad \beta_4 = \alpha-\beta. \tag{16}$$

The FID law of the nondiagonal element $\rho_{nm}(t)$ of the coupled system's reduced density matrix ρ thus has the form

$$F_{nm}(t) = \frac{\rho_{nm}(t)}{\rho_{nm}(0)} = \left\langle \exp i \int_0^t d\tau [(\alpha_n - \alpha_m) q_1^2(\tau) + (\beta_n - \beta_m) q_2^2(\tau)] \right\rangle_P, \tag{17}$$

where $\langle\cdots\rangle_P$ denotes the average over all possible stochastic process of the fluctuations [3,33].

Direct calculation of Eq. (17) is complicated by the correlation between $q_1(t)$ and $q_2(t)$. To simplify this problem, we make the linear cross approximation. This approximation states that there exist a standard spectral function $S(\omega)$ and three constants $\{a,b,\gamma\}$ such that [20]

$$S_{11}(\omega) = \int_{-\infty}^{\infty} \langle \delta n_{g1}(t)\, \delta n_{g1}(t-\tau)\rangle_B e^{i\omega\tau} d\tau = a^2 S(\omega), \tag{18}$$

$$S_{22}(\omega) = \int_{-\infty}^{\infty} \langle \delta n_{g2}(t)\, \delta n_{g2}(t-\tau)\rangle_B e^{i\omega\tau} d\tau = b^2 S(\omega), \tag{19}$$

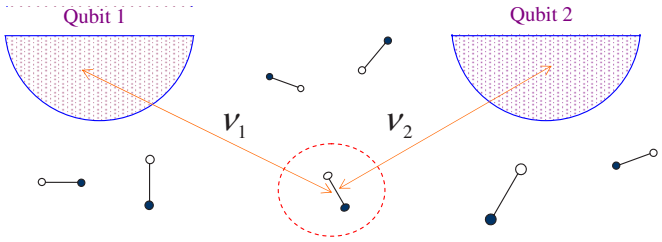

FIG. 2. (Color online) Schematic sketch of the charged TLFs near the coupled qubits.

$$S_{12}(\omega) = \int_{-\infty}^{\infty} \langle \delta n_{g1}(t)\, \delta n_{g2}(t-\tau)\rangle_B e^{i\omega\tau} d\tau = ab\gamma S(\omega), \tag{20}$$

$$S_{21}(\omega) = \int_{-\infty}^{\infty} \langle \delta n_{g2}(t)\, \delta n_{g1}(t-\tau)\rangle_B e^{i\omega\tau} d\tau = ab\gamma S(\omega). \tag{21}$$

The LCA is partially inspired by the present reported experimental results. For example, $S(\omega)$ could be selected as the ubiquitous $1/\omega$ spectrum in solid-state physics; thus Eqs. (18) and (19) suggest that both qubits suffer $1/\omega$ type noise; in addition, the assumptions Eqs. (20) and (21) are supported by the detected approximative linear dependence of $S_{12}(\omega)$ on $S_{11}(\omega)$ and $S_{22}(\omega)$ in Ref. [20] with $\gamma = 0.15 \pm 0.05$.

We can also interpret the LCA from the microscopic point of view [4]. In the system we consider, the origin of the low-frequency charge noise can be regarded as the sum of a noninteracting TLF ensemble broadly distributed in the background [5,6,23,34], each fluctuator of which is characterized by its switching rate Γ and coupling strength to the two CPBs ν_1 and ν_2, as shown in Fig. 2. In the high-temperature limit [9], the self-cross-power spectra of $\delta n_{g1}(t)$ and $\delta n_{g2}(t)$ are

$$S_{11}(\omega) = \int\int d\nu_1 d\Gamma\, P(\nu_1,\Gamma) \frac{\nu_1^2 \Gamma}{\omega^2+\Gamma^2}, \tag{22}$$

$$S_{22}(\omega) = \int\int d\nu_2 d\Gamma\, P(\nu_2,\Gamma) \frac{\nu_2^2 \Gamma}{\omega^2+\Gamma^2}, \tag{23}$$

$$S_{12}(\omega) = S_{21}(\omega) = \int\int d(\nu_1\nu_2) d\Gamma\, P(\nu_1\nu_2,\Gamma) \frac{\nu_1\nu_2\Gamma}{\omega^2+\Gamma^2} \tag{24}$$

where $P(\ldots)$ denotes the distribution functions of the particular variables.

In single-electron nanocircuits, the physics of the TLF ensemble is often conjectured as thermal-activated hopping of electrons in a localized bistable potential well or as charge traps on a surface near the gate electrodes [35]. The switching rate Γ of a TLF in the ensemble is usually determined by the width or height of its localized potential barrier, while the coupling strengths ν_1 and ν_2 depend on their location. In disordered systems, it is generally assumed that the distribution of the TLF's location (and thus the coupling strengths ν_1, ν_2) and its switch rate Γ are independent, i.e., the distribution functions $P(\nu,\Gamma)$ in Eqs. (22)–(24) have the factorized form

$$P(\nu,\Gamma) = P(\nu)P(\Gamma). \tag{25}$$

Therefore, the forms of the four spectra S_{ij} are identical because all of them are determined by the same integral $\int P(\Gamma)[\Gamma/(\omega^2+\Gamma^2)]d\Gamma$.

We move on by defining the functions

$$U_1(t) = \frac{1}{2\cos\varphi}\left(\frac{\delta n_{g1}(t)}{a} + \frac{\delta n_{g2}(t)}{b}\right),$$

$$U_2(t) = \frac{1}{2\sin\varphi}\left(\frac{\delta n_{g1}(t)}{a} - \frac{\delta n_{g2}(t)}{b}\right), \tag{26}$$

where the angle φ satisfies $\cos 2\varphi = \gamma$. One can easily prove that $U_1(t)$ and $U_2(t)$ are "normalized" and uncorrelated:

$$\int_{-\infty}^{\infty} \langle U_1(t)U_1(t-\tau)\rangle_B e^{i\omega\tau} d\tau = \int_{-\infty}^{\infty} \langle U_2(t)U_2(t-\tau)\rangle_B e^{i\omega\tau} d\tau = S(\omega), \tag{27}$$

$$\int_{-\infty}^{\infty} \langle U_2(t)U_1(t-\tau)\rangle_B e^{i\omega\tau} d\tau = \int_{-\infty}^{\infty} \langle U_1(t)U_2(t-\tau)\rangle_B e^{i\omega\tau} d\tau = 0. \tag{28}$$

In this way, Eq. (17) becomes

$$F_{nm}(t) = \left\langle \exp i \int_0^t d\tau [A_{nm}U_1^2(t) + B_{nm}U_2^2(t) + 2C_{nm}U_1(t)U_2(t)] \right\rangle_P, \tag{29}$$

where the parameters A_{nm}, B_{nm}, and C_{nm} are inferred from Eqs. (6), (15), (16), and (26). For the real symmetric matrix

$$M_{nm} = \begin{bmatrix} A_{nm} & C_{nm} \\ C_{nm} & B_{nm} \end{bmatrix} \tag{30}$$

we denote λ_{1nm}, λ_{2nm} as its eigenvalues and its unitary Jordan matrix $J_{nm} = (J_{nm})_{ij}$ as

$$M_{nm} = J_{nm}^{\dagger} \begin{bmatrix} \lambda_{1nm} & 0 \\ 0 & \lambda_{2nm} \end{bmatrix} J_{nm}. \tag{31}$$

Therefore

$$A_{nm}U_1^2(t) + B_{nm}U_2^2(t) + 2C_{nm}U_1(t)U_2(t) = \lambda_{1nm}W_{1nm}^2(t) + \lambda_{2nm}W_{2nm}^2(t), \tag{32}$$

where

$$\begin{bmatrix} W_{1nm}(t) \\ W_{2nm}(t) \end{bmatrix} = J_{nm} \begin{bmatrix} U_1(t) \\ U_2(t) \end{bmatrix}. \tag{33}$$

Just like $U_1(t)$ and $U_2(t)$, $W_{1nm}(t)$ and $W_{2nm}(t)$ are also normalized and uncorrelated; therefore $F_{nm}(t)$ can be factorized as

$$F_{nm}(t)=\left\langle \exp\left(i\int_0^t d\tau \lambda_{1nm} W_{1nm}^2(\tau)\right)\right\rangle_P \times\left\langle \exp\left(i\int_0^t d\tau \lambda_{2nm} W_{2nm}^2(\tau)\right)\right\rangle_P . \quad (34)$$

Equation (34) indicates that we can directly get the decay law of coupled qubits from the already known results for single-qubit dephasing. One specific example is that both qubits of the coupled system are exposed to transverse Gaussian $1/f$ noise $[S(\omega)=1/\omega]$. From its single-qubit correspondence [7], we write $F_{nm}(t)$ as

$$|F_{nm}(t)|=\left[1+\left(\frac{2}{\pi}\lambda_{1nm}t\ln\frac{1}{\omega_{ir}t}\right)^2\right]^{-1/4} \times\left[1+\left(\frac{2}{\pi}\lambda_{2nm}t\ln\frac{1}{\omega_{ir}t}\right)^2\right]^{-1/4}, \quad (35)$$

where ω_{ir} is the infrared cutoff of the $1/f$ noise.

IV. DYNAMICAL DECOUPLING IN COUPLED CPBs

Since decoherence in Josephson circuits is dominated by strong low-frequency noise, the dynamical decoupling technique (also called spin-echo or bang-bang control), already used in the field of nuclear magnetic resonance (NMR), appears to be particularly promising [3] in prolonging the coherence time. For the above coupled-qubit system, before discussing the efficiency of dynamical decoupling we should first consider its feasibility. We summarize the local operation resources we can achieve from operators:

$$R_1=\frac{1}{\sqrt{2}}(\sigma_{x1}+\sigma_{x2}) =\begin{bmatrix} 0 & 0 & \cos\theta+\sin\theta & 0\\ 0 & 0 & \cos\theta-\sin\theta & 0\\ \cos\theta+\sin\theta & \cos\theta-\sin\theta & 0 & 0\\ 0 & 0 & 0 & 0\end{bmatrix}, \quad (36)$$

$$R_2=\frac{1}{\sqrt{2}}(\sigma_{x1}-\sigma_{x2}) =\begin{bmatrix} 0 & 0 & 0 & \cos\theta-\sin\theta\\ 0 & 0 & 0 & -\cos\theta-\sin\theta\\ 0 & 0 & 0 & 0\\ \cos\theta-\sin\theta & -\cos\theta-\sin\theta & 0 & 0\end{bmatrix}. \quad (37)$$

It is thus suitable to use charge-type ac local gate pulses to selectively address transitions between the four states [8,9,32]. For example, to complete a population inversion between states $|1\rangle$ and $|3\rangle$, which we label as Π_{13}, we can apply an ac pulse of R_1 resonant with the transition frequency $\omega_{13}=|E_{10}-E_{30}|$. In the interaction picture, the evolution of the system is governed by [9]

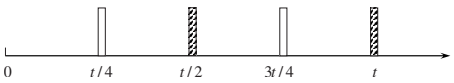

FIG. 3. Dynamical decoupling pulses in the coupled system. The hollow rectangles represent the operation $\Pi_{13}\otimes\Pi_{24}$ and the shaded are for operations $\Pi_{14}\otimes\Pi_{23}$.

$$H_{ac}(t)=g\widetilde{R_1}(t)(e^{i\omega_{13}t}+\text{H.c.}), \quad (38)$$

where the g factor denotes the Rabi frequency, typically on the level of 100 MHz, and $\tilde{R}_1(t)$ is the representation of R_1 in the interaction picture:

$$\widetilde{R_1}(t)=[(\cos\theta+\sin\theta)e^{-i\omega_{13}t}|1\rangle\langle 3|+(\cos\theta-\sin\theta)e^{-i\omega_{23}t}|2\rangle \times\langle 3|]+\text{H.c.} \quad (39)$$

Suppose the g factor is much smaller than $|\omega_{13}-\omega_{23}| =2E\sin 2\theta$; at time $t_0=\pi/[4g(\cos\theta+\sin\theta)]$ we get

$$\exp\left(-i\int_0^{t_0}H_{ac}(\tau)d\tau\right)\cong|1\rangle\langle 3|+|3\rangle\langle 1|=\Pi_{13}, \quad (40)$$

while the $|2\rangle\leftrightarrow|3\rangle$ is suppressed by the large detuning $2E\sin 2\theta$ [36]. The other unforbidden interlevel population inversions Π_{14}, Π_{23}, and Π_{24}, can be similarly realized.

Any random phase noise in the four-dimensional Hilbert space of coupled qubits can be decomposed into linear addition of the following three operators (the trivial identity operator has been omitted):

$$N_1=\begin{pmatrix}1&0&0&0\\0&1&0&0\\0&0&-1&0\\0&0&0&-1\end{pmatrix},\quad N_2=\begin{pmatrix}1&0&0&0\\0&-1&0&0\\0&0&1&0\\0&0&0&-1\end{pmatrix},\quad N_3=\begin{pmatrix}1&0&0&0\\0&-1&0&0\\0&0&-1&0\\0&0&0&1\end{pmatrix}. \quad (41)$$

To dynamically decouple N_1-type noise, we only need to perform Π_{13} and Π_{24} synchronously. In the same way, the noise N_2 and N_3 could also be dynamically decoupled.

A schematic diagram of the dynamical decoupling pulses is depicted in Fig. 3. The evolution of ρ_{nm} in the presence of these pulses could be evaluated from Eq. (34) and previous spin-echo results for a single pulse [23]:

$$F_{Enm}(t)=\frac{\rho_{Enm}(t)}{\rho_{nm}(0)}\cong\left[1+\frac{1}{2}\left(\frac{\lambda_{1nm}t}{2\pi}\right)^2(\omega_c t)^2\ln\frac{\omega_c}{\omega_{ir}}\right]^{-1/2} \times\left[1+\frac{1}{2}\left(\frac{\lambda_{2nm}t}{2\pi}\right)^2(\omega_c t)^2\ln\frac{\omega_c}{\omega_{ir}}\right]^{-1/2}, \quad (42)$$

where the subscript E denotes the word "echo" and ω_c is the ultraviolet cutoff of the $1/f$ noise. One should notice that Eq. (42) is an approximate result because in the pulse sequence of Fig. 3, N_1 has been decoupled twice while both N_2 and N_3

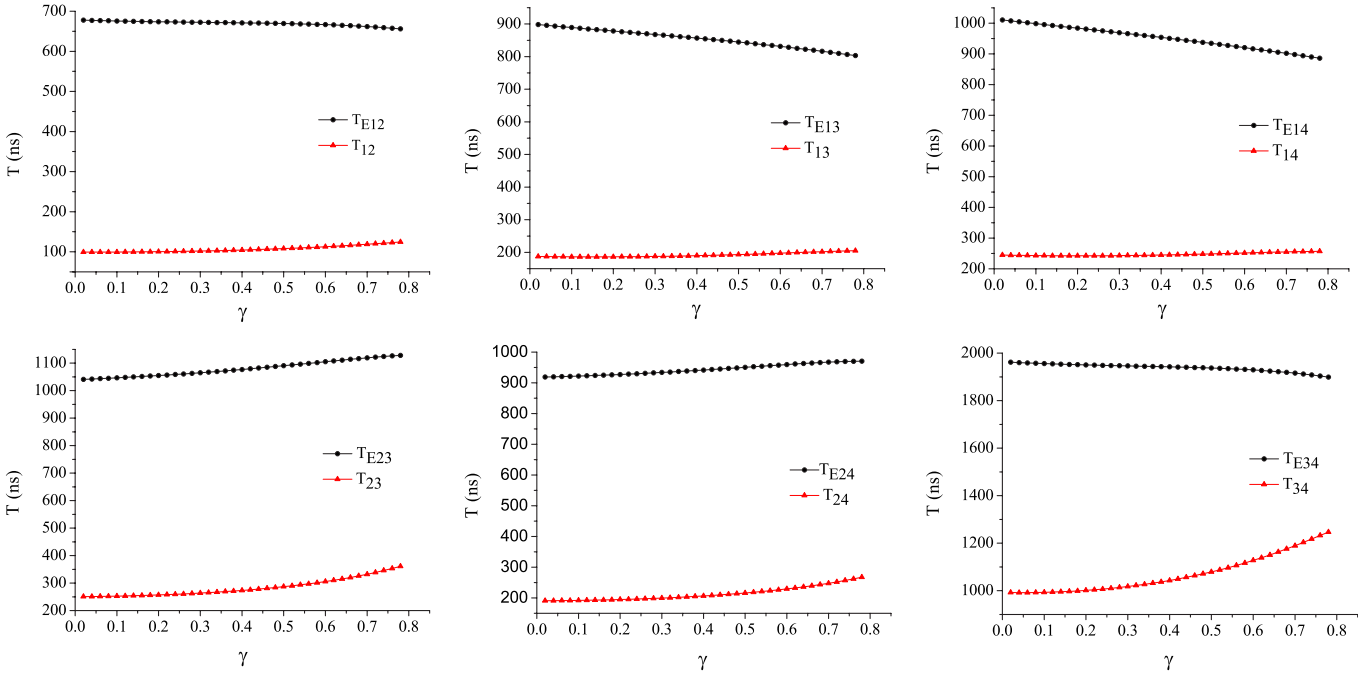

FIG. 4. (Color online) FID decay times and dynamical decoupling decay times of each nondiagonal matrix element of the coupled system's density matrix. The circles represent the decay times when bang-bang pulses as shown in Fig. 3 are injected, while the triangles represent the FID case.

have been decoupled once, i.e., Eq. (42) *overestimates* the decoherence to some extent.

V. NUMERICAL RESULTS

The decoherence times of $F_{nm}(t)$ and $F_{Enm}(t)$ versus the noise correlation factor γ have been plotted in Fig. 4. As shown in Eqs. (35) and (42), neither the FID nor the dynamical decoupling decay is exponential; thus the dephasing times $T_{nm}(T_{Enm})$ are defined by $F_{nm}(T_{nm})=1/e$ or $F_{Enm}(T_{Enm})=1/e$. The parameters we use are selected based on reported experimental data: for the coupled qubits, we choose $E_J=E_c=16.4$ GHz and $E_m=0.06E_J$, while for the noise sources, we set two identical noise sources with $a=b=1.3\times10^{-3}$ s/rad and cutoff frequencies $\omega_{ir}=2\pi\times1$ Hz, $\omega_c=2\pi\times0.4$ MHz.

From Fig. 4 we can see the dephasing times are generally of the order 0.1 μs, on the same level as the observed single-qubit dephasing time [8,9]. One may find that the efficiency of dynamical decoupling in our calculation is higher than the experimental data [3,9]. This can be attributed to the omission of the nearly white noise from the gate bias and the high-frequency tails of the $1/f$ noise [21,37].

One important result is that the quadratic dephasing times depend weakly on the noise correlation factor γ. In some previous proposals, it has been suggested that the correlation of the noise sources, whether intrinsic or coupling induced [10,11], could be used to construct DFS; hence the coherence of some particular states could be protected. However, this method is valid only for longitudinal dephasing. Even if the linear longitudinal qubit-noise coupling is completely eliminated by the collective environment, the quadratic dephasing still exists. From this point of view, we may conclude there are still many problems left in suppressing the decoherence of superconducting circuits by the encoding method.

VI. DISCUSSION AND CONCLUSION

Before concluding we offer a remark about the correlation factor γ. The previous common and uncorrelated noise models could be viewed as the zero-order expression for the noise correlation. In this sense, our introduction of the factor γ is a first-order correction. However, it is clear that just this rough factor cannot contain all the details of the noise spatial correlation. Hence we expect a more refined formalism in further study of decoherence in coupled qubits.

One point we should emphasize is that our method is applicable only if the decoherence process could be completely described by the spectra of noises. As shown in Sec. III, the LCA is deduced from the following two basic assumptions of the Dutta-Horn model: (i) the low-frequency noise is the sum of many RTNs; (ii) for these RTNs, the distributions of their coupling strengths and switch rates are factorized. In most realizations of Josephson charge qubits, these two assumptions prove to be correct. However, in recent research on single-qubit decoherence, in addition to the observation of conventional Gaussian $1/f$ noise [3,21], some novel phenomena such as sample-to-sample effects and non-Gaussian noise have also been demonstrated [9], i.e., in some experiments, single-qubit decoherence cannot be fully determined from the information about the noise spectrum. Physically speaking, this anomaly could be traced back to the qubit-TLF interaction mechanism. In some particular experimental setup (e.g., the material of the substrate in which the

TLFs are embedded), the influence from a few strongly coupled TLFs (which are located nearest to the qubit) on the single-qubit dephasing exceeds that from the other many but weakly coupled TLFs. For the small number of the strongest TLFs, the concept of a statistical distribution function becomes meaningless. From the mathematical point of view, the peculiar qubit-TLF interaction form may lead to a singular distribution function $P(v)$ of the coupling strength v between the fluctuators of the TLF ensemble and the qubit, which makes the standard central limit theorem break down [34]. For example, if we attribute the TLFs to the structural defects behaving as elastic dipoles that interact with the qubit via a deformational potential, we will get a distribution function $P(v) \propto 1/v^2$ which provides divergence variance [6]. In this situation, the detailed statistics of the noise source becomes important in the single-qubit decoherence. For the coupled-qubit system here, the Gaussian $1/f$ noise case has been considered, while the understanding of more general situations requires exploration in the future.

In conclusion, in this paper we consider the quadratic dephasing of capacitively coupled CPBs exposed to partially correlated low-frequency charge noise. With the help of a reasonable approximation, we calculate the dephasing rate versus the spatial correlation of the environment for Gaussian $1/f$ noise. We also discuss realizing dynamical decoupling in the coupled system with present technology. This work may offer improvement in preserving the quantum coherence of solid-state systems.

ACKNOWLEDGMENTS

Y.H. thanks T. Tu, Y. J. Han, and X. B. Zou for their inspiration and fruitful discussion. This work was funded by the National Fundamental Research Programs No. 2006CB921900 and No. NCET-04-0587, Innovation funds from the Chinese Academy of Sciences, and the National Natural Science Foundation of China (Grant Nos. 60621064 and No. 10574126).

[1] Y. Makhlin, G. Schon, and A. Shnirman, Rev. Mod. Phys. **73**, 357 (2001).
[2] M. H. Devoret, A. Wallraff, and J. M. Martinis, e-print arXiv:cond-mat/0411174.
[3] Y. Nakamura, Y. A. Pashkin, T. Yamamoto, and J. S. Tsai, Phys. Rev. Lett. **88**, 047901 (2002).
[4] P. Dutta and P. M. Horn, Rev. Mod. Phys. **53**, 497 (1981).
[5] E. Paladino, L. Faoro, G. Falci, and R. Fazio, Phys. Rev. Lett. **88**, 228304 (2002).
[6] Y. M. Galperin, B. L. Altshuler and D. V. Shantsev, Phys. Rev. Lett. **96**, 097009 (2006).
[7] Y. Makhlin and A. Shnirman, Phys. Rev. Lett. **92**, 178301 (2004).
[8] D. Vion, A. Aassime, A. Cottet, P. Joyez, H. Pothier, C. Urbina, D. Esteve, and M. H. Devoret, Science **296**, 886 (2002).
[9] G. Ithier, E. Collin, P. Joyez, P. J. Meeson, D. Vion, D. Esteve, F. Chiarello, A. Shnirman, Y. Makhlin, J. Schriefl, and G. Schon, Phys. Rev. B **72**, 134519 (2005).
[10] X. Zhou, M. Wulf, Z. Zhou, G. Guo, and M. Feldman, Phys. Rev. A **69**, 030301(R) (2004).
[11] J. Q. You, X. D. Hu, and F. Nori, Phys. Rev. B **72**, 144529 (2005).
[12] M. Governale, M. Grifoni, and G. Schon, Chem. Phys. **268**, 273 (2001).
[13] M. J. Storcz and F. K. Wilhelm, Phys. Rev. A **67**, 042319 (2003).
[14] M. J. Storcz, U. Hartmann, S. Kohler, and F. K. Wilhelm, Phys. Rev. B **72**, 235321 (2005).
[15] M. Thorwart and P. Hanggi, Phys. Rev. A **65**, 012309 (2002).
[16] J. M. Cai, Z. W. Zhou, and G. C. Guo, Phys. Rev. A **74**, 022328 (2006).
[17] D. I. Tsomokos, M. J. Hartmann, S. F. Huelga, and M. B. Plenio, New J. Phys. **9**, 79 (2007).
[18] F. Bloch, Phys. Rev. **105**, 1206 (1957).
[19] A. J. Leggett, S. Chakravarty, A. T. Dorsey, Matthew P. A. Fisher, Anupam Garg, and W. Zwerger, Rev. Mod. Phys. **59**, 1 (1987).
[20] A. B. Zorin, F. J. Ahlers, J. Niemeyer, T. Weimann, H. Wolf, V. A. Krupenin, and S. V. Lotkhov, Phys. Rev. B **53**, 13682 (1996).
[21] O. Astafiev, Y. A. Pashkin, Y. Nakamura, T. Yamamoto, and J. S. Tsai, Phys. Rev. Lett. **93**, 267007 (2004).
[22] J. Bergli, Y. M. Galperin, and B. L. Altshuler, Phys. Rev. B **74**, 024509 (2006).
[23] J. Schriefl, Ph.D. thesis, Universitat Karlsruhe (TH), 2005 (unpublished).
[24] Y. A. Pashkin, T. Yamamoto, O. Astafiev, Y. Nakamura, D. V. Averin, and J. S. Tsai, Nature (London) **421**, 823 (2003).
[25] T. Yamamoto, Y. A. Pashkin, O. Astafiev, Y. Nakamura, and J. S. Tsai, Nature (London) **425**, 941 (2003).
[26] Y. Nakamura, Yu. A. Pashkin, and J. S. Tsai, Nature (London) **398**, 786 (1999).
[27] Y. Makhlin, G. Schon, and A. Shnirman, Nature (London) **398**, 305 (1999).
[28] M. H. Devoret, in *Quantum Fluctuations*, edited by S. Reynaud, E. Giacobino, and J. Zinn-Justin, Proceedings of the Les Houches Summer School of Theoretical Physics, LXIII (Elsevier, Amsterdam, 1997), p. 351.
[29] J. Siewert, R. Fazio, G. M. Palma, and E. Sciacca, J. Low Temp. Phys. **118**, 795 (2000).
[30] J. Siewert and R. Fazio, Phys. Rev. Lett. **87**, 257905 (2001).
[31] M. Tinkham, *Introduction to Superconductivity*, 2nd ed. (McGraw-Hill, New York, 1996).
[32] A. Cottet, Ph.D. thesis, Universite Paris VI, 2002 (unpublished).
[33] G. Ithier, Ph.D. thesis, Universite Paris VI, 2005 (unpublished).
[34] J. Schriefl, Y. Makhlin, A. Shnirman, and G. Schon, New J. Phys. **8**, 1 (2006).
[35] R. Bauernschmitt and Y. V. Nazarov, Phys. Rev. B **47**, 9997 (1993).
[36] A. Blais, A. Maassen van den Brink, and A. M. Zagoskin, Phys. Rev. Lett. **90**, 127901 (2003).
[37] A. Shnirman, G. Schon, I. Martin, and Y. Makhlin, Phys. Rev. Lett. **94**, 127002 (2005).